

MEASURING THE FORCES THAT CONTROL PROTEIN INTERACTIONS

Deborah Leckband

*Department of Chemical Engineering and the Center for Biophysics and Computational Biology, University of Illinois at Urbana-Champaign, Urbana, Illinois 61801;
e-mail: leckband@uiuc.edu*

Key Words molecular forces, force probes, receptor, intermolecular potentials, unfolding

■ **Abstract** Although the force fields and interaction energies that control protein behavior can be inferred indirectly from equilibrium and kinetic measurements, recent developments have made it possible to quantify directly (a) the ranges, magnitudes, and time dependence of the interaction energies and forces between biological materials; (b) the mechanical properties of isolated proteins; and (c) the strength of single receptor-ligand bonds. This review describes recent results obtained by using the atomic force microscope, optical tweezers, the surface force apparatus, and micropipette aspiration to quantify short-range protein-ligand interactions and the long-range, nonspecific forces that together control protein behavior. The examples presented illustrate the power of force measurements to quantify directly the force fields and energies that control protein behavior.

CONTENTS

INTRODUCTION	2
FORCES IN BIOLOGICAL INTERACTIONS	3
Nonspecific Interactions	3
Specific Interactions	4
Net Interaction Profiles—The Principle of Superposition	5
TECHNIQUES FOR PROBING MOLECULAR FORCES	6
Atomic Force Microscope and Optical Tweezers	6
Surface Force Apparatus	7
Micropipette Aspiration/Bioforce Probe	8
MAPPING THE ELECTROSTATIC PROPERTIES OF PROTEIN SURFACES	8
FORCES CONTROLLING THE RECOGNITION OF IMMOBILIZED RECEPTORS	10
Short-Range Steric Barriers and the Accessibility of Immobilized Receptors	11
Polymer Surface Barriers and Selective Binding	11
Long-Range Electrostatic Forces	13
Dynamic Properties of Surface-Bound Receptors	13

MEASURING THE STRENGTHS OF RECEPTOR-LIGAND BONDS	14
Theoretical Interpretation of the Forces to Rupture Single Bonds	14
The Tensile Strengths of Single Bonds Depend on the Activation Energy for Unbinding	16
Mechanical Properties of Proteins	17
Simulations of Forced Unbinding—Relating Rupture Forces to Bond Chemistry . .	19
INTERACTIONS INVOLVING MULTIPLE INTERMOLECULAR BONDS	20
Multiple Bonds in Parallel	20
The Rupture of Bonds in Series	21
Multivalent Protein Interactions	21

INTRODUCTION

Protein interactions with ligands, other proteins, or surfaces are controlled by a complex array of intermolecular and intersurface forces. Soluble antibody binding to cell surface antigens, for example, involves specific, lock-and-key interactions, which are mediated by multiple hydrogen bonds, van der Waals interactions, and hydrophobic and steric contacts within the antibody-binding site. To focus on only the binding site, however, neglects the important influence of several nonspecific electrostatic, van der Waals, and steric forces that operate outside the binding pocket between the antibody surface and the target membrane. These forces are superimposed on the lock-and-key interaction and can alter not only the binding kinetics but also the equilibrium distribution of receptor-ligand bonds. This interplay of specific and nonspecific forces controls all protein interactions ranging from bimolecular collisions in solution to adhesion between cells.

The forces that control protein behavior and their physical chemical origins are typically inferred indirectly from equilibrium binding and kinetic measurements or are calculated with molecular models. From changes in association rates caused by site-directed mutations, for example, one might infer the contribution of charged amino acids to the long-range receptor-ligand forces. Alternatively, calculated energies are used to identify the role of physical chemical interactions in protein function and behavior. Although detailed calculations are feasible for small molecules, such calculations become prohibitive with the increasing size and complexity of biological macromolecules and their state of aggregation, the number of solvent molecules involved, and the range of the interactions.

Time-dependent forces between soft or mobile species add yet another degree of complexity. Because of the importance of dynamics in biology, static models of intermolecular or intersurface interactions do not describe the full range of parameters that influence biological behavior. Some computational approaches such as Brownian dynamics simulations do address these issues, but they are subject to the accuracy of the force fields used and have limited applications. A goal of many biophysical studies is to determine the molecular forces that control biological interactions and to use this information to rationally manipulate, for

example, protein function. This capability is currently limited by our inability to quantitatively link molecular architecture, composition, and dynamics to the force fields that govern the behavior of complex biological molecules such as proteins.

Force measurements provide powerful means of directly quantifying the complex interactions that determine the properties of biological molecules and biomaterials. With the recent, rapid development of several force probes, one can now measure directly (a) the ranges, magnitudes, and time dependence of the interaction energies and forces between materials; (b) the mechanical properties of isolated proteins; and (c) the strength of single receptor-ligand bonds. The combination of these measurement techniques with (a) structural information, (b) the ability to construct well-defined model systems, and (c) computer simulations has made it possible to establish quantitatively how the composition, architecture, and dynamics govern interactions in biology.

Biological force measurements encompass many different measurement techniques. This review focuses, in particular, on approaches that (a) quantify directly the ranges, magnitudes, and dynamics of forces in protein interactions and (b) elucidate the detailed relationships between chemistry, molecular structure, physical chemistry of bond formation or rupture, and bond energetics. We first consider measurements of the specific and the nonspecific forces that together control protein behavior. The review then focuses on force measurements of single proteins and the theoretical developments that recently clarified how such forces relate to the protein bond chemistry. The final section addresses multivalent protein interactions and the use of force measurements to establish how these interactions differ from those of single, isolated protein-ligand bonds. Together, the examples presented illustrate the power of direct measurements to identify the fundamental forces that control protein interactions.

FORCES IN BIOLOGICAL INTERACTIONS

Nonspecific Interactions

Electrostatic Double-Layer Force The electrostatic double-layer force between charged particles is one of the principal long-range forces that govern biological interactions. In aqueous solutions, the charges on the particle surface are balanced by an electrical double layer of ions in solution. This layer increases the ion concentration in the gap between the interacting particles relative to the bulk solution. The resulting osmotic pressure between the surfaces is the basis of the repulsive (or attractive) “double-layer” force (32). Except at small separations, it decays exponentially with the distance D as $e^{-\kappa D}$, where κ^{-1} is the Debye screening length. The latter depends on the solution dielectric constant and the ion concentration (32). The surface charge density determines the counterion concentration near the surface and hence the magnitude of the double-layer force. This

force also depends on geometry. For example, between a spherical probe tip and a flat surface, the magnitude scales with the tip radius R (32).

Van der Waals Force The van der Waals force is the second important long-range interaction in biology. Between atoms and small molecules, the force decays as $1/D^7$. However, between a larger sphere of radius R and a flat surface, for example, the force is $F = -\frac{AR}{6D^2}$, and it is longer ranged (32). One consequence of this longer range is that the nonspecific van der Waals force between the tip of a force probe and the sample can contribute to the apparent forces between molecules bound to those surfaces.

In the above expression, A , the Hamaker constant, scales the magnitude of the force between the materials (32). This parameter depends on the polarizability of atoms and on the refractive indices and the dielectric constants of the interacting materials, as well as the medium between them. Therefore, depending on the media, the van der Waals force can be attractive or repulsive (32). Its exact distance dependence does depend on geometry, and between a sphere and a flat surface, the magnitude also scales with the radius of the sphere (32).

“Steric” Forces Repulsive forces between surface-anchored polymeric materials operate at intermediate separations, that is, 1–10 nm, the range of which is generally determined by the molecular weight and grafting density of the polymer. Cell surfaces and some biomaterials are coated with a dense layer of water-soluble polymers, which present a repulsive barrier that prevents the close approach of two particles or the diffusion of soluble molecules to the underlying surface. These forces are entropic in origin and depend on temperature but not ionic strength.

Steric repulsion operates at short intermolecular separations. This force is caused by the overlap of electron clouds, and the resulting repulsion is a consequence of the Pauli exclusion principle (32). There is no theoretically defined distance dependence for this force. However, the dimensions of the interacting species determine the range, and the decay is described empirically by a $1/D^{12}$ power law. This distance dependence is independent of temperature and of the ionic strength.

Specific Interactions

Specific interactions refer to a particular class of highly complementary, noncovalent bonds between molecules. Crystal structures of protein-ligand complexes exhibit the high degree of shape and chemical complementarity typical of molecular recognition. Owing to the multiple van der Waals, hydrogen-bonding, and hydrophobic contacts that stabilize the interaction, the binding free energy can be large. However, these interactions are determined by the local geometry, and they typically lock in when the ligands are docked, that is, within 1–2 nm. There are examples in which the electrostatic potential fields caused by charges in the binding sites extend over much larger distances (70). In general, however, the potential

may be deep relative to the thermal energy kT , but the width tends to be narrow and the interaction short ranged.

Net Interaction Profiles—The Principle of Superposition

Any protein interaction will be governed by a superposition of some or all of these different forces. The net interaction force profile (or potential) can therefore be a complicated function with multiple minima and maxima (Figure 1). The distance dependence and magnitudes of the force profiles govern both protein association kinetics and the equilibrium-binding behavior. In terms of the corresponding energies, the deepest minimum determines the thermodynamic stability of complexes, and the potential profile at larger separations modulates the association rates (29).

Protein interactions are clearly not determined solely by their specific binding sites. However, both the magnitudes and distance dependencies of the force (or energy) profiles are required to identify the different interactions responsible for protein behavior. These factors can be determined by measuring directly the distance-dependent force profiles between the materials of interest. One can further

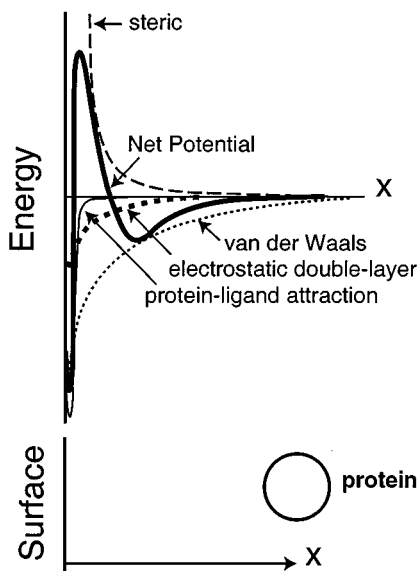


Figure 1 Hypothetical interaction potential between a soluble protein and a surface. The net potential profile (*bold solid line*) is a superposition of the van der Waals potential (*dotted line*), attractive or repulsive double-layer potential (*bold dashed line*), steric repulsion (*long dashed line*), and specific, short-range interactions (*solid line*). The relative ranges and magnitudes of these interactions can give rise to complicated potentials that exhibit multiple minima and energy barriers.

identify the contributing interactions by measuring changes in the profiles caused by changes in temperature and solution conditions (29, 32).

Some of the techniques discussed in this review can measure distance-dependent force (or energy) profiles. Other techniques lack the requisite distance resolution but are sufficiently sensitive to quantify single bond strengths. With the best distance resolution of ± 0.1 nm, the fine structure of short-ranged lock-and-key potentials still cannot be mapped directly. It is possible to quantify changes in bond rupture kinetics in response to applied stress. Additionally, a recent strategy enabled investigators to detect energy barriers along the unbinding pathway of a ligand in the binding site of a protein. These methodologies offer a comprehensive toolbox with which to probe the variety of forces and energies that govern protein function.

TECHNIQUES FOR PROBING MOLECULAR FORCES

With the current force probes, one can now quantify forces between biological materials that range from 0.01 pN to 10 nN. The principal techniques used to investigate proteins are the atomic force microscope (AFM) (Figure 2*a*) (90), surface force apparatus (SFA) (Figure 2*b*) (31), bioforce probe (BFP) (Figure 2*c*) (18), and optical tweezers (OT) (Figure 2*d*) (71, 77).

In addition to the direct force probes shown in Figure 2*a–d*, shear flow detachment assays have been used to determine the strengths of protein bonds and the dynamic responses of bonds to stress (1, 37, 79). With this approach, one measures the fluid shear stress required to detach a cell or beads from a chemically modified substrate. From the determined force, the geometry of the cell or sphere, and the receptor density, one can determine the average strength of the adhesive bonds.

Atomic Force Microscope and Optical Tweezers

The AFM uses a silicon nitride probe mounted on a soft cantilever spring to measure the force between the probe tip with a radius of ~ 10 – 50 nm and a second surface. This instrument has been used extensively to image soft biological materials with a lateral resolution of ± 1 nm. As the tip approaches the test material, the cantilever deflects under the influence of the net force between the surfaces, and forces of 1–1000 pN can be measured. The position of a laser beam reflected off the cantilever surface tracks the relative movements of the probe within ± 0.1 nm and records the spring deflection. The sample separation is inferred indirectly from the cantilever displacement relative to the apparent position of steric, that is, hard wall contact between the materials.

The OT uses the radiation pressure focused on a 1- to 2- μ m bead to exert very small forces (1–200 pN) against molecules or materials interacting weakly with the bead (71, 77). The bead is visualized in the optical trap, and the substrate or a second bead to which it is bound is moved relative to the trap position. By varying the force exerted on the optically trapped bead, one can determine the

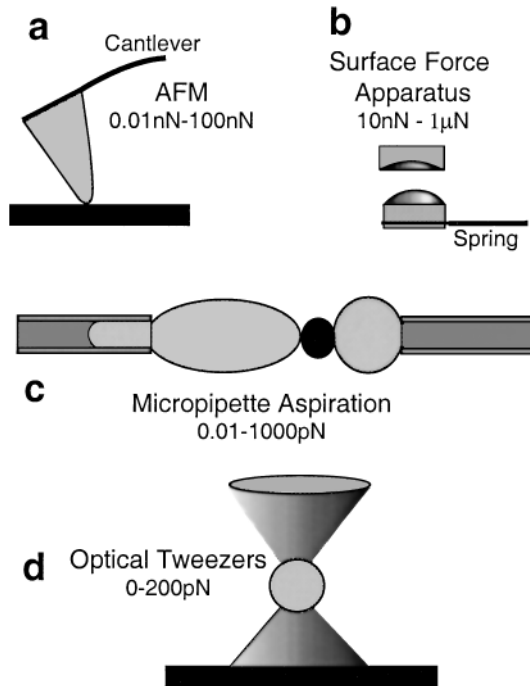


Figure 2 Force probes used to directly measure protein interaction forces. *a.* The atomic force microscope, showing the probe tip attached to the cantilever force transducer. *b.* The surface force apparatus, showing the crossed cylinders (2-cm radii) of the apparatus and the force-transducing spring. *c.* The bioforce probe, consisting of a membrane capsule aspirated into a pipette. A bead (*center*) is attached to one membrane (*left*), and the force between the bead and a second capsule or glass bead (*right*) is exerted by aspirating the (*left*) membrane into the pipette. *d.* Optical tweezers. The bead is held in the optical trap, and the radiation pressure exerted on the bead opposes adhesive contacts between materials on the bead and surface.

force necessary to break the weak bonds. Although force-distance profiles cannot be measured accurately, OTs—because of their sensitivity—have been used to measure the force-extension profiles of soft, entropic springs such as titin (38, 81), as well as the force-velocity relationships of molecular motors (71).

Surface Force Apparatus

With the SFA (31), one measures the force as a function of the separation distance between materials bound to two crossed cylinders with 1- to 2-cm radii of curvature. This approach differs from many others because the probed regions are large, for example, $1\text{--}5\ \mu\text{m}^2$, and typically reflect an average of $>10,000$ molecular interactions. These interactions collectively give rise to a sufficiently

large force to be measured with a sensitive leaf spring that supports one of the samples. An important point is that this geometry in fact allows one to measure the free energy between the materials directly. This consequence results from the Derjaguin approximation, which relates the force between materials on two crossed cylinders to their interaction energy (29, 32). The interaction energy—not the force—determines equilibrium protein behavior. With the SFA, one measures this energy directly. Whereas the force resolution of ± 10 nN is lower than that of the other instruments (see below), weak interactions caused by, for example, van der Waals forces are routinely measured.

An advantage of this method is the optical interferometric technique used to measure the intersurface distances. The sample materials are within the resonant cavity of an interferometer, so that changes in the distance between the materials shift the wavelengths of the interference fringes. From the wavelength shifts, one determines *in situ* the surface separations with a resolution of ± 0.1 nm. This resolution is independent of surface deformations or the compression of soft materials between the layers. The shapes of the fringes also reflect the shape of the contact region, and local surface deformations are visualized *in situ*. During measurements, one can therefore determine distance between samples, extent of surface contact, shape of the contact region, and lateral heterogeneity with ± 1 - μm resolution in the surface topology (31). With the SFA, one obtains the most accurate force-distance profiles of the current measurement techniques.

Micropipette Aspiration/Bioforce Probe

The micropipette aspiration technique is used to measure the force between a membrane bag, for example, an erythrocyte, and giant vesicles, cells, or, more recently, functionalized beads (18). The adhesion between the membranes is determined from micromechanical analyses of the global deformations of the membrane capsules, which are held in contact by suction at the tips of opposed micropipettes. The force transducers are soft membrane capsules rather than mechanical springs, and the membrane tension controls the transducer stiffness. With a measurable range of from 0.01 pN to ~ 1000 pN, this approach can probe the widest range of forces accessible with a single instrument.

The more recent configuration, the BFP, uses reflectance interference contrast microscopy to determine the distances between the bead and substrate, with a resolution of ~ 5 nm (18). The use of a bead attached to the erythrocyte transducer (Figure 2c) made distance measurements possible, and it significantly expanded the number of systems accessible for study with this approach.

MAPPING THE ELECTROSTATIC PROPERTIES OF PROTEIN SURFACES

In solution, the long-range electrostatic forces between proteins and other molecules are important determinants of protein behavior. In particular, the distribution of charges on protein surfaces and the resulting asymmetric electrostatic fields are

believed to modulate ligand association rates, catalytic rates, and redox potentials (21, 28, 41, 85). The electrostatic fields are thought to enhance association rates by preorienting charged reactants. For example, DNA-binding proteins, such as the processivity factor of *Escherichia coli* DNA polymerase III, are net negatively charged, but the DNA-binding domain contains a localized patch of positive charge (45).

Although difficult to measure directly, electrostatic surface potentials of proteins can be calculated by using mean field approaches and the crystal structures of the macromolecules (28, 53, 85). These methods have been extremely valuable for interpreting biochemical data in terms of the influences of structure on protein function. Calculated protein electrostatic potentials are also used in Brownian dynamics simulations to model protein association kinetics (28, 53). However, the simulation results depend on the electrostatic models used and on the underlying assumptions of these models. The calculated intermolecular potentials often involve adjustable parameters such as solvation energies, the protein dielectric constants, and the variation of the solvent dielectric with the intermolecular distances (53, 85). Given these uncertainties, recent efforts have focused on developing scanning-probe methods for obtaining electrostatic maps of protein surfaces by direct measurements.

AFM images of charged patches on patterned surfaces demonstrated the feasibility of mapping charge distributions at high resolution (26). The repulsive forces between a charged molecule or surface and the AFM tip are caused by both steric repulsion and the electrostatic double-layer force between the surfaces. The variation of the tip-sample repulsion reflects the surface topography with a lateral resolution of ± 1 nm.

Steric forces are ionic strength independent, and one can, in principle, quantify the double-layer force based on salt-dependent changes in the repulsive forces. Two groups thus mapped the relative spatial variations of the local charge densities on protein surfaces from differences in the force contours measured at various ionic strengths (26, 57). From the measured changes in the repulsive forces with changes in the salt concentration, they obtained a qualitative map of the protein surface charge density. The ability to obtain accurate quantitative data is, however, limited by the uncertainty in the distance between the probe tip and the protein surface and in the curvature of the probe tip, which scales the force (32).

An alternative approach used the SFA to probe protein electrostatics. Rather than resolving lateral features on the protein surface, the investigators manipulated the orientation of the immobilized protein so that all proteins in a monolayer exposed the identical surface. The average electrostatic surface properties of the monolayer and of the adjacent electrostatic double-layer are then determined primarily by the outermost charged amino acid residues. Fits of the measured double-layer force between the protein monolayer and a "test surface" of known charge to solutions of the Poisson-Boltzmann equation yield the average electrostatic potential of the outer protein surface (46, 48). The optical interferometric technique of the SFA made possible accurate determinations of the

protein-probe surface separation (± 0.2 nm), the local radius of curvature of the probe, and hence the measured, average charge density of the exposed protein surface (31).

Such surface force measurements performed with immobilized, oriented Fab' fragments of monoclonal, antiluorescein antibodies demonstrated that a cluster of positive charges surrounding the binding site attracts the negatively charged antigen fluorescein (46). These qualitative results provided direct evidence for the role of charge clusters in guiding ligand-docking trajectories, despite the net negative charges on both molecules.

Recently, Sivasankar et al (76) used the SFA to quantify the pH-dependent charge density on a single face of immobilized, oriented streptavidin. To do this, they measured the average charge density of the exposed protein surface as a function of the solution pH. The measured point of zero charge differed by ~ 1.5 pH units from the isoelectric point of the soluble protein. This finding confirmed that the measured double-layer force reflects local electrostatic fields on the exposed surface of the macromolecule and not the overall protein charge.

The comparison of these results with mean field electrostatic calculations, which accounted for these pH-dependent changes, verified that the measured charge densities on the streptavidin surface exhibited the predicted pH dependence. The surface-averaged charge densities, determined from the calculated three-dimensional electrostatic potential distribution, agreed quantitatively with results from the force measurements (76). These experimental and computational results show therefore that coarse-grained electrostatic potential maps of the protein exterior can be determined directly using (a) surface force measurements and (b) the controlled manipulation of the immobilized protein orientation.

FORCES CONTROLLING THE RECOGNITION OF IMMOBILIZED RECEPTORS

Nonspecific forces also affect recognition events at interfaces. In many examples, such as hormone binding to cell surface receptors and drug targeting, the surface microenvironment can alter the apparent kinetics and/or thermodynamics of protein recognition events. In such cases, the force profiles that control receptor binding are a superposition of specific receptor-ligand interactions and nonspecific forces between the soluble ligand and the substrate (cf Figure 1). Changes in the net force (or potential) profile can perturb the distribution of bound and free states; the rates of ligand binding (2); and, in cell adhesion, both the contact area and the membrane separation at equilibrium (5, 80). Direct measurements of the force-distance curves can identify the different forces that govern protein interactions at surfaces. Such studies have been used to quantify, for example, the impact of grafted polymers and polymer dynamics on these events.

Short-Range Steric Barriers and the Accessibility of Immobilized Receptors

Close to surfaces ($D < 2$ nm), short-range forces can affect the recognition of small, surface-bound molecules. In particular, near hydrated bilayers, repulsive forces caused by out-of-plane lipid fluctuations, the motion of chemical groups, and adsorbed water can extend ≤ 1 –2 nm (32, 33). This range is often comparable with both the dimensions of small, tethered receptors and the depth of the protein-binding sites. As a result, these repulsive forces can counter the specific bonds between the bound receptors and soluble ligands. This interference can be avoided by tethering receptors via long spacers, which position the receptors beyond most steric surface barriers and allow them to fully penetrate the protein-binding pockets.

With the SFA, Leckband et al (46) quantified the effect of short-range hydration/fluctuation forces on binding between the Fab' fragment of an anti fluorescein antibody and membrane-bound fluorescein. They related reductions in the receptor-ligand adhesion directly to measured changes in the ranges of short-ranged repulsive surface barriers. By immobilizing the fluorescein antigen with spacers of different lengths, these investigators used the tethers as molecular rulers to control the distance between the receptor and the surface (46). Although the antibody-binding pocket is 1.8 nm deep, to achieve the maximum adhesion, they required at least a 2.3- to 2.5-nm tether (46). The additional 0.5–0.7 nm needed was attributed to the repulsive hydration/fluctuation forces, which decreased the effective spacer length. The measured 0.7 ± 0.1 -nm range of these repulsive forces confirmed this interpretation.

Polymer Surface Barriers and Selective Binding

Longer-ranged surface forces (1–10 nm) caused by surface-bound polymers prevent or modulate the binding of soluble molecules to immobilized receptors. Absent direct protein binding to cell surface carbohydrates or to polymers, the latter large molecules can prevent protein access to surface-bound molecules (*a*) by resisting the compression of the chains or (*b*) by preventing protein penetration of the layers. Investigations of the influence of such barriers on protein adsorption have focused on synthetic, water-soluble polymers owing to their biotechnological importance. Nevertheless, although there are important differences between them, synthetic, linear polymers and cell surface carbohydrates are expected to hinder molecule or particle interactions with surfaces by qualitatively similar mechanisms.

The energy penalty for compressing end-anchored polymers (brushes) by soluble proteins was first modeled by Jeon et al (36). This scenario can occur when the distance between chain-anchoring sites is less than the protein radius (25). Direct measurements of the forces between streptavidin monolayers and end-grafted polyethylene oxide (PEO) chains tested this model directly. Of particular interest are the dependencies of the ranges and magnitudes of the steric barriers on the polymer molecular weight and grafting density. Sheth & Leckband (72) found

that the range and distance dependence of the repulsion were as predicted by theories for polymer brushes (36). They also measured weak attraction between the protein and the PEO (72), the outcome of which was in contrast to expectations. It is important that, although they did show that simple polymer theories describe some properties of this polymer, these direct measurements (*a*) identified deviations from ideal behavior and (*b*) revealed the limitations of simple theories for describing the full range of PEO interactions with proteins. Such investigations are not limited to PEO but can be conducted with other polymers and proteins.

Soluble proteins can also penetrate polymer layers when the spacing between the chain-anchoring sites exceeds the protein diameter. In this case, the osmotic penalty for protein insertion into the layer opposes its diffusion through the chains (25, 78). Using micropipette aspiration, Noppl-Simson & Needham (59) quantified the osmotic barrier for avidin binding to biotin receptors beneath grafted polymers. They used polyethylene oxide bound to large, unilamellar vesicles, which also contained lipid-anchored biotin. From the work to induce adhesion between the latter vesicles and avidin-coated vesicles, they determined that the osmotic penalty for avidin penetration of the polymer film was roughly consistent with that estimated with the polymer surface density and protein size (25, 59, 78).

Grafted chains also sterically impede particle aggregation and receptor-mediated cell adhesion. Coating blood-borne drug carriers with PEO, for example, prevents their rapid uptake by the liver and prolongs their circulation time (61). Kennedy and coworkers (39) showed similarly that, by tuning the balance of the streptavidin-biotin attraction and polymer repulsion between vesicles, they could control the vesicle aggregation rates and the aggregate structures that formed. In cell adhesion studies, the degree of cell spreading on surfaces displaying adhesion peptides could be tuned by adjusting the length of the surrounding grafted polymers (13). Chan & Springer (7) similarly showed that increasing the length of the lymphocyte function-associated antigen-3 adhesion protein increased the attachment efficiency of lymphocytes displaying the adhesion protein CD2 onto lymphocyte function-associated antigen-3-transfected cells.

In these examples the balance between protein-ligand attraction and steric repulsion between membrane-anchored polymers determines the net intermembrane adhesion. Determination of the magnitudes and ranges of the forces exerted provides mechanistic information regarding the forces that determine the biological behavior. Alternatively, to manipulate the interactions, we need to know how the range and the magnitude of the repulsion depend on the polymer identity, molecular weight, and surface density (43). Again, direct-force measurements can directly test whether simple theories for grafted chains accurately predict the properties of real polymers.

To investigate the mechanism of vesicle stabilization by grafted PEO, for example, the distance dependence of the repulsive forces between lipid bilayers with grafted chains was quantified by two different approaches (43, 58). The results confirmed that the polymer barrier sterically stabilizes the vesicles. Further, by showing that simple polymer theories describe the repulsion between PEO brushes, the measurements also confirmed that, with PEO, such theories can be

used to generate design criteria for stabilizing vesicles or tuning receptor-mediated cell adhesion (13).

Extending these measurements to cell surface carbohydrates should similarly clarify the role of these biopolymers in regulating biological activity. For example, the posttranslational modification of the neural cell adhesion molecule by polysialic acid, a linear polyelectrolyte, has been linked to neural plasticity in the early stages of development (67). Force measurements between neural cell adhesion molecule monolayers with and without polysialic acid would quantify the impact of this modification on the protein function and directly test various models for the biological activity of this carbohydrate.

Long-Range Electrostatic Forces

Force probes have similarly been used to quantify the effects of long-range electrostatic forces on biological interactions. In particular, these tests have determined (a) the forces responsible for the altered affinities of immobilized receptors (87, 88) and (b) the ranges and magnitudes of competing receptor-ligand attraction and electrostatic repulsion (46, 48). Shear detachment studies also demonstrated the effects of electrostatics on receptor-ligand bond formation and rupture in cell adhesion (68).

Dynamic Properties of Surface-Bound Receptors

In previous sections, we treated the surface-bound molecules as static structures. They are, however, soft materials that undergo thermally excited fluctuations. The lateral mobility of molecules on fluid cell surfaces can also lead to time-dependent intermembrane potentials. For example, using the SFA, Leckband et al (48) measured the time dependence of nonequilibrium forces between membranes that were associated with the dynamics of lateral receptor diffusion and ligand-receptor binding.

Tethered receptors bound via longer anchors can undergo large fluctuations, which can be quantified by similar time-dependent measurements of force-distance profiles. Such receptors are common in biology, in cases where the binding sites of cell surface molecules extend away from the bilayer surface and the glycocalyx. In addition, polymer conjugates are used to anchor receptors to drug-delivery agents such as liposomes. The flexible anchors can undergo thermally excited fluctuations. As a result, the receptor-ligand potential is distributed over a continuum of states that are a function of the parameters that control the tether mobility. The resultant intersurface potential, or the potential of mean force, is then an ensemble-averaged distortion of the intrinsic receptor-ligand potential. The ligand mobility thus smears the potential over a much greater range than would be exhibited by the rigidly bound molecule.

Surface force measurements between tethered biotin and an immobilized, oriented streptavidin monolayer (Figure 3) demonstrated directly the effects of such ligand dynamics on intersurface potentials (86). When bound via a flexible PEO tether, the distribution of biotin near the surface was determined by the large

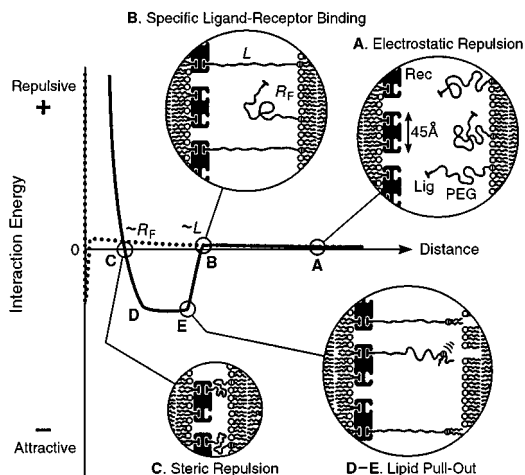


Figure 3 Interaction potential between tethered biotin and streptavidin. At A, the surfaces experience electrostatic repulsion. The protein and ligand lock in at B, as a result of the large fluctuations of the tethered biotin, and then jump in to C. Upon separation, the streptavidin and biotin remain bound (C, D, and E) until the polymer is stretched, and the lipids anchoring the polyethylene oxide pull out of the membrane (E). The dotted line shows the interaction potential between streptavidin and biotin anchored directly to the membrane. Reproduced from reference 86 with permission.

fluctuations of the chain. Although the average thickness of the polymer brush was 3.5 nm, the tethered biotin end-groups can undergo large, rapid excursions from the mean polymer thickness. Using the SFA, these investigators measured the distance dependence and the dynamics of the intersurface interactions. In contrast to the short-range attraction measured between streptavidin and lipid-anchored biotin (Figure 3) (27, 48), PEO-tethered biotin bound streptavidin readily at distances up to two thirds of the fully extended polymer chain length (Figure 3) (86). The increased range of the biotin-streptavidin potential is a direct consequence of the thermal fluctuations of the PEO tether. Without both the distance and the force resolution, these measurements would not be possible. These studies open up exciting possibilities for exploring the impact of chain stiffness, polymer molecular weight, and grafting density both on the polymer fluctuations and on receptor-ligand potentials.

MEASURING THE STRENGTHS OF RECEPTOR-LIGAND BONDS

Theoretical Interpretation of the Forces to Rupture Single Bonds

The measured nonspecific forces considered thus far are well understood theoretically, but the potential energy surfaces that govern specific recognition are less

well characterized. The recent use of force probes to rupture single receptor-ligand bonds suggested that such measurements might in fact be used to probe the details of protein-ligand potentials. One expects that the forces to induce bond failure can be readily interpreted in terms of certain properties of the bonds. Bell, over 20 years ago (4), first proposed a relationship between the bond rupture forces and both the intermolecular potentials of stressed bonds and the kinetics of bond failure. Applying the kinetic theory of the strength of solids to receptor-ligand bond failure, he predicted that the external force applied to the bond would increase the detachment rate and that the bond strength would depend on the gradient of the binding free energy (4).

The effect of an applied mechanical force f on the potential $E(x)$ of an unstressed bond is illustrated in Figure 4. Owing to ambient thermal noise, there is a finite probability that the unperturbed bonds (Figure 4a) will acquire sufficient energy to overcome the activation barrier $E(x_{ts})$ at the transition state x_{ts} and will dissociate spontaneously. However, the application of a force f at an angle θ relative to the bond axis distorts the net potential by $-f\cos\theta$ (Figure 4a). This distortion lowers the activation barrier relative to kT at x_{ts} , increases the probability of barrier crossings, and thereby increases the frequency of bond rupture.

Measurements of cell detachment kinetics as a function of the shear stress on attached cells first demonstrated the decrease in bond lifetimes with increasing

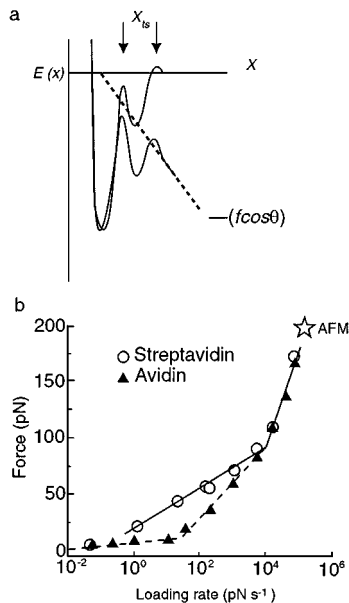


Figure 4 Effect of applied mechanical force on receptor-ligand unbinding. *a.* The application of a mechanical potential $-f\cos\theta$ on the receptor-ligand potential $E(x)$ tilts the potential and lowers the activation energy $E(x_{ts})$ at the transition state x_{ts} . *b.* The different slopes of the streptavidin- and avidin-biotin rupture force vs the logarithm of the loading rate. Reproduced with permission from reference 55.

applied load. Alon et al (1) showed that the rupture of bonds between glycoproteins on activated neutrophils and immobilized selectins increased with increasing fluid shear stress. A similar approach was used to study the lifetimes of bonds between receptor-coated beads and ligand-coated substrates (61, 62). The dissociation rate both of antibody-antigen and of CD2-CD48 (T-cell adhesion proteins) bonds also increased with increasing shear stress (61, 62).

Recently, Evans & Ritchie expanded on Bell's model in a rigorous theoretical model of induced bond failure (16). This analysis makes the important point that the apparent bond rupture force is the force to induce bond failure in a defined time interval. They used Kramers' rate theory (42) to describe the detachment of mechanically stressed receptor-ligand bonds. Their analysis predicts an increased rupture frequency with the applied load, and the dependence of the apparent rupture force on the observation time. Within this framework are three dynamic unbinding regimes, which are defined by the relative loading and intrinsic bond dissociation rates. First, in the slow-loading regime, the rate at which the bonds are stressed is slower than the intrinsic dissociation rate. The linkages will break spontaneously before any appreciable force is applied, and the force to induce bond failure tends to zero. In the intermediate regime, the force relaxation rate is of the same order of magnitude as the intrinsic relaxation rate of the bond, and the apparent bond strength varies with the loading velocity. In both of the latter cases, receptor-ligand unbinding is thermally activated. In the forced-unbinding regime, however, the applied load reaches the maximum bond strength faster than spontaneous dissociation occurs, and the rupture force reflects the maximum bond strength.

Using the BFP and two unrelated proteins, Merkel et al (55) and Simson et al (74) verified the predictions of the Evans & Ritchie model. With avidin and biotin, Merkel et al (55) showed that the apparent bond strength indeed varies with the loading velocity (Figure 4*b*). At rapid loading rates, the analysis also predicts the crossover between spontaneous and force-induced unbinding. With avidin and biotin, the force vs loading-rate curves did not reach the maximum bond strength $F_b = E_b / X_{ts}$. This may be because the experimental methods cannot achieve the rapid rates required (16, 18). Recent studies of the breakage of immunoglobulin G (IgG)-protein A bonds did exhibit crossover from spontaneous to force-activated unbinding (74).

The Tensile Strengths of Single Bonds Depend on the Activation Energy for Unbinding

The model proposed by Evans & Ritchie (16) predicts that the bond rupture kinetics are controlled by the activation energy for unbinding. By contrast, Bell's analysis assumed that the applied mechanical potential must overcome the binding free energy ΔG . Later arguments similarly proposed that the rupture force would depend logarithmically on the affinity (12). Indeed, measurements of antibody-antigen bond strengths, determined by using shear flow detachment assays, exhibited the predicted logarithmic dependence on affinity (44).

The first AFM studies of the forces to break bonds between streptavidin and different biotin analogs did not, however, correlate with the binding free energy ΔG (49, 56). Instead they varied linearly with the equilibrium enthalpy of the bond ΔH (56). A later, elegant study with streptavidin mutants demonstrated that the critical force to break the streptavidin-biotin linkage depends on the activation enthalpy ΔH^\ddagger for unbinding (9). In this case, the energy barrier for unbinding and hence the rupture force is determined primarily by the activation enthalpy. The activation entropy ΔS^\ddagger , which is related to the width of the potential and the distribution of bound states (22, 35), may contribute in other systems, but it is apparently negligible for streptavidin-biotin bond rupture.

The groups using the AFM analyzed receptor-ligand unbinding in terms of the transition state theory for reaction rates (19, 49, 56). This approach is not inconsistent with the theoretical model proposed by Evans & Ritchie (16). Although there are important distinctions between transition state theory and Kramers' rate theory, both approaches describe the reactions in terms of an activation barrier with a finite width (22, 35, 42). Kramers' theory reduces to transition state theory in the low viscosity limit—that is, when the viscous drag on the ligand is small (42).

The dependence of the rupture forces on the activation energy for unbinding suggests the possibility of mapping the energy landscapes of receptor-ligand potentials. The BFP studies with avidin detected three different dynamic regimes of the rupture force (Figure 4*b*). These regimes were attributed to the three major energy barriers along the unbinding trajectory that were identified in prior molecular dynamics simulations (Figure 4*a*) (16, 34). As the mechanical force tilts the net potential surface, the outer barriers are lowered to $<kT$, and each of the inner barriers emerges in succession to dominate the unbinding kinetics (Figure 4*a*). Detecting all three barriers, however, required measurements at loading rates that spanned 5–6 orders of magnitude (55)!

Force probes have already been used to detect qualitative changes in protein interactions caused by site-directed mutagenesis or cofactor binding. For example, AFM measurements detected changes in protein interactions that alter insulin crystallization behavior after site-directed mutagenesis (89). Differences in protein interactions with the chaperone GroEL were also measured in the presence and absence of ATP (83). The challenge now is to determine how such changes affect the potential energy surfaces mapped by dynamic force measurements.

Mechanical Properties of Proteins

There are many reports of force probe measurements of the mechanical properties of proteins. The majority of them address the mechanico-chemical transduction of motor proteins and the relationship between structure, catalysis, and force transduction. Several excellent reviews have been written that describe this body of work (40, 54, 71, 77), and we do not duplicate those efforts here. However, we focus on the recent use of force probes to investigate both the structural and the

functional aspects of force-induced distortions of protein structure. Proteins are stabilized by multiple noncovalent interactions, and the disruption of these bonds by either mechanical or chemical means induces protein unfolding. Direct measurements have therefore been used to investigate the forces that stabilize protein structures and to determine how they affect the mechanical properties of isolated proteins.

The first investigations of mechanically induced unfolding were done with titin (38, 65, 66, 81). This protein is a scaffold for thick-filament formation, and it determines the elasticity of relaxed, striated muscle. It comprises multiple, tandem repeats of IgG- and fibronectin III-like domains, and its force-extension profiles were measured both with the AFM and with OT (38, 65, 66, 81). The AFM measurements exhibited periodic spikes in the force-extension curve that were attributed to the reversible unfolding transitions of the individual domains (65) (Figure 5). The sharpness of the peaks suggested that the protein unfolded by a two-state mechanism (65).

The force curves alone cannot identify the chemical mechanisms responsible for the peaks, that is, transition states in the extension profiles. However, molecular dynamics simulations (see below) suggest that the rupture of hydrogen bonds between two antiparallel strands of the beta sheet of the Ig domains generates the force to induce domain unfolding and hence the peaks in the force-extension curves (50, 51). Differences between the AFM and laser tweezers data suggest that the force-extension profiles depend on both the unfolding chemistry and the measurement method, that is, the sample history (38, 65, 81). Whereas the AFM curves display a sequence of periodically spaced peaks, the tweezers data exhibit a broad, extensible region from which domain unraveling was inferred (38). This difference was recently rationalized in terms of the different loading rates. An extension of the earlier model of Evans & Ritchie (16) described

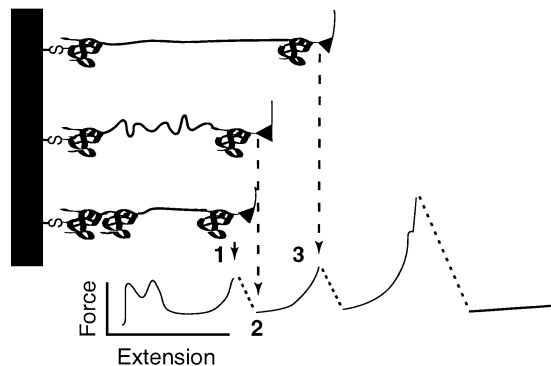


Figure 5 Forced unfolding of titin. The successive unfolding of titin domains gives rise to the corresponding peaks and valleys in the force-extension profile measured with the atomic force microscope (*bottom*). Reproduced with permission from reference 65.

the rupture of bonds attached to soft tethers and accounted for these differences in terms of the intrinsic unfolding reaction rates relative to the loading dynamics (17).

The dependence of bond rupture characteristics on loading rates was used to test whether the transition state in the forced unfolding pathway was the same as for protein unfolding in solution. By changing the rate of pulling, Carrion-Vazquez and coworkers (6) estimated the unfolding kinetics of a polypeptide consisting of multiple Ig domains in tandem. Comparing the measured kinetics to Monte Carlo simulations gave the unfolding rate in the absence of force. The quantitative agreement between the rates thus determined and those measured in solution strongly supports the hypothesis that the events that generate the peaks in the force curve are the same as those responsible for the transition state in the unfolding pathway of the soluble protein (6).

Although there are only a few molecular mechanics investigations of known structural proteins, recent reports suggest that forced protein deformations may play a broader role in biology. The molecular dynamics simulation of forced fibronectin unfolding suggests that the resulting encryption of the RGD sequence may act as a mechanical recognition switch (50, 51). That this function may regulate the biological activity of extracellular matrix proteins is suggested by studies that show differential fibronectin activities on different substrata (20). In addition, a recent study of the chaperone protein GroEL suggests that the latter may actually facilitate protein folding by stretching misfolded or partially folded proteins (73).

Simulations of Forced Unbinding—Relating Rupture Forces to Bond Chemistry

Supercomputers have made it possible to simulate the unbinding trajectories of ligands as they are pulled over the rugged energy landscape of the binding pocket. The first such study sought to identify the physical chemical interactions that determine the unbinding force for avidin-biotin bond rupture. Simulations of the forced rupture of the bond between biotin and a monomer of the tetrameric protein streptavidin reproduced quantitatively the measured detachment force (23).

The natural tendency would be to use such steered molecular dynamics (SMD) simulations to interpret single-bond detachment data in terms of the chemical interactions and simulated energy barriers that control unbinding. The obstacle to such quantitative comparisons lies in the different time scales on which intermolecular dissociation is induced in the experimental versus the computational approaches (3, 34). Experimentally measured dissociation events occur on millisecond time scales and are thermally activated. By contrast, the nanosecond time scales used in molecular dynamics simulations are fast relative to the intrinsic relaxation time of the bond. To induce bond dissociation in the simulations, very large forces must be applied rapidly to overcome all potential barriers on such short time scales. Under these conditions, there is a substantial frictional contribution to the pull-off force that scales with the detachment velocity. This term is large relative to the

applied load, and for this reason, the simulations overestimate the experimental values significantly (3, 34). Not only do the frictional terms differ in these two limits, but the rupture force also scales differently with the applied load (3).

The amount of irreversible work performed in the simulations is the principle obstacle to quantitative comparisons between SMD results and force probe measurements. The error in the potential surface reconstructed from simulations is related to the irreversible work performed during bond rupture (3). Potential surfaces cannot be reconstructed quantitatively from force probe measurements, which record thermally activated events (3). Recent theoretical developments suggest that the results from these two approaches can be bridged through a potential of mean force (24). The latter can be constructed through time-series analyses of the position and applied force data obtained from calculated SMD trajectories (24). The thus determined potential of mean force can then be used to interpret force probe measurements in terms of the energy peaks and valleys that control receptor-ligand unbinding.

Simulated unbinding trajectories already identified key molecular interactions that prevent protein unfolding and limit the escape or determine the binding pathways of ligands. They provided important information regarding, for example, retinal binding to bacterio-opsin (30) and the forced unfolding of proteins (50, 51). Other results guided the interpretation of experimental measurements of avidin-biotin bond rupture (55). These examples illustrate the value of combining theoretical approaches and force probe measurements. SMD promises to be a powerful tool for interpreting bond rupture measurements.

INTERACTIONS INVOLVING MULTIPLE INTERMOLECULAR BONDS

Multiple Bonds in Parallel

Biological adhesion is not typically mediated by single, high-affinity interactions, but by many weak contacts. The advantage of the latter is that weak interactions allow for plasticity in adhesive junctions, the formation of dynamic contacts, and cell motility (11, 14, 15, 52, 60). Because low-affinity bonds are believed to exhibit short lifetimes and low rupture forces, adhesion requires multiple such interactions (62, 82).

To investigate how the rupture of multiple contacts might differ from single-bond failure, Vijayendran and associates (84) used the adhesive dynamics algorithm (8) to simulate the adhesion between receptor-linked surfaces in surface force measurements. At equilibrium, there will be a distribution of bound and free states, and the average bond strength will be less than that of isolated cross bridges. However, the materials remain pinned in close proximity by the unbroken, neighboring cross bridges, and broken bonds can reform. Because of this, the time-averaged tension on each bond during the junction rupture can approach and

even exceed the critical rupture force of the individual bonds. This effect will be most prevalent when the intrinsic breakage and reformation rates are faster than the loading rate (84). Such behavior will not be observed in single-bond measurements because the surfaces jump out of contact when the cross bridges fail. The adhesive dynamics simulations thus show that, with multiple contacts in parallel, the adhesion is determined by the unbinding kinetics, the loading rate, and the reassociation kinetics.

The Rupture of Bonds in Series

Adhesive interactions can also involve several bonds in series. For example, receptor-mediated cell-cell contacts that involve cytoskeletal interactions may involve five or more bonds in series. One predicts that the average strength of such linkages would be lower than any of the individual linkages. If the binding probability of each of two different bonds in series is less than unity, then the probability that both bonds will exist simultaneously is the product of the probabilities of each of the constitutive bonds. The overall likelihood of simultaneous binding will then be less than that of either individual bond (69).

This hypothesis was confirmed by radial flow detachment assays of cross-bridges formed by two low-affinity bonds. These studies showed that the average bond rupture force was 2- to 10-fold smaller than that of the weakest bond in the series (69). On the other hand, with linkages comprising four high-affinity bonds, surface force measurements demonstrated that the bond with the lowest rupture force failed first (47). The force-extension curves of titin suggest similarly that the domains with the lowest activation barrier to unfolding unravel first (65). The affinities do influence the adhesion by determining the probability of cross-bridge formation. However, the force to rupture the existing cross bridges is determined (a) by the bond in the series with the lowest activation barrier to unbinding and (b) by the loading dynamics relative to the intrinsic unbinding rates (16).

Multivalent Protein Interactions

Other proteins such as fibronectin may bind more than one ligand simultaneously or have multiple binding sites for single ligands. Many cell adhesion molecules contain large, multidomain extracellular segments (10), and some exhibit multiple contacts with their corresponding ligands (64). Whereas multiple interactions may contribute to binding, their implications for protein-mediated adhesion have not been explored.

A recent study identified one possible consequence of such interactions. The extracellular domain of an adhesion protein cadherin consists of five homologous domains in tandem and binds to identical proteins on opposing cell surfaces. With the force apparatus, Sivasankar et al (75) found that cadherin extracellular domains bind in at least two antiparallel configurations. By controlling the distance between two cadherin monolayers, they identified two discrete protein separations at which the proteins adhere. The force-distance profile generated during protein

detachment suggests that the sequential rupture of these bonds may hinder the abrupt failure of the cadherin junctions (75).

Whether other adhesion proteins undergo similar multidomain interactions or bind in more than one configuration remains to be determined. In addition, the functional consequences of such interactions have yet to be explored. Direct force measurements will be essential tools for quantifying the tensile strengths of the linkages and determining the mechanisms by which the proteins bind and resist adhesive failure.

ACKNOWLEDGMENTS

I thank A Halperin, K Schulten and S Sivasankar for their helpful comments. This work was supported by NIH GM51338 and NSF BES 9503045 CAREER.

Visit the Annual Reviews home page at www.AnnualReviews.org

LITERATURE CITED

- Alon R, Hammer DA, Springer TA. 1995. Lifetime of the P-selectin-carbohydrate bond and its response to tensile force in hydrodynamic flow. *Nature* 374:539–42
- Balgi G, Leckband D, Nitsche JM. 1995. Transport effects on the kinetics of protein-surface binding. *Biophys. J.* 68:2251–60
- Balsera M, Stepaniants S, Izrailev S, Oono Y, Schulten K. 1997. Reconstructing potential energy functions from simulated force-induced unbinding processes. *Biophys. J.* 73:1281–87
- Bell GI. 1978. Models for the specific adhesion of cells to cells. *Science* 200:618–27
- Bell GI, Dembo M, Bongrand P. 1984. Cell adhesion: competition between nonspecific repulsion and specific bonding. *Biophys. J.* 45:1051–64
- Carrien-Vazquez M, Oberhauser AF, Fowler SB, Marszalek PE, Broedel SE, et al. 1999. Mechanical and chemical unfolding of a single protein: a comparison. *Proc. Natl. Acad. Sci. USA* 96:3694–99
- Chan P, Springer TA. 1992. Effect of lengthening lymphocyte function associated antigen 3 on adhesion to CD2. *Mol. Biol. Cell* 3:157–76
- Chang K-C, Hammer DA. 1996. Influence of direction and type of applied force on the detachment of macromolecular-bound particles from surfaces. *Langmuir* 12:2271–82
- Chilkoti A, Boland T, Ratner BD, Stayton PS. 1995. The relationship between ligand-binding thermodynamics and protein-ligand interaction forces measured by atomic force microscopy. *Biophys. J.* 69:2125–30
- Chothia C, Jones EY. 1997. The molecular structure of cell adhesion molecules. *Annu. Rev. Biochem.* 66:823–62
- Davis MM. 1995. Serial engagement proposed. *Nature* 375:104
- Dembo M, Torney DC, Saxman K, Hammer D. 1988. The reaction-limited kinetics of membrane-to-surface adhesion and detachment. *Proc. R. Soc. London Ser. B* 234:55–83
- Dori Y, Bianco-Peled H, Satija SK, Fields GB, McCarthy JB, Tirrell M. 2000. Ligand accessibility as a means to control cell response to bioactive bilayer membranes. *Langmuir*. Submitted
- Dustin ML. 1997. Adhesive bond dynamics in contacts between T lymphocytes and glass-supported planar bilayers

- reconstituted with the immunoglobulin-related adhesion molecule CD58. *J. Biol. Chem.* 272:15782–88
15. Dustin ML, Golan DE, Zhu D-M, Miller JM, Meier W, et al. 1997. Low-affinity interaction of human or rat T cell adhesion molecule CD2 with its ligand aligns adhering membranes to achieve high physiological affinity. *J. Biol. Chem.* 272:30889–98
 16. Evans E, Ritchie K. 1997. Dynamic strength of molecular adhesion bonds. *Biophys. J.* 72:1541–55
 17. Evans E, Ritchie K. 1999. Strength of a weak bond connecting flexible polymer chains. *Biophys. J.* 76:2439–47
 18. Evans E, Ritchie K, Merkel R. 1995. Sensitive force technique to probe molecular adhesion and structural linkages at biological interfaces. *Biophys. J.* 68:2580–87
 19. Florin E-L, Moy VT, Gaub HE. 1994. Adhesion forces between individual ligand-receptor pairs. *Science* 264:415–17
 20. Garcia A, Vega MD, Boettinger D. 1999. Modulation of cell proliferation and differentiation through substrate-dependent changes in fibronectin conformation. *Mol. Biol. Cell* 10:785–98
 21. Getzoff E, Cabelli D, Fisher C, Parge H, Viezzoli M, et al. 1992. Faster superoxide dismutase mutants designed by enhancing electrostatic guidance. *Nature* 358:347–51
 22. Glasstone S, Laidler K, Eyring H. 1941. *The Theory of Rate Processes*. New York: McGraw-Hill
 23. Grubmüller H, Heynman B, Tavan P. 1996. Ligand binding: molecular mechanics calculation of the streptavidin-biotin rupture force. *Science* 271:997–99
 24. Gullingsrud JR, Braun R, Schulten K. 1999. Reconstructing potentials of mean force through time series analysis of steered molecular dynamics simulations. *J. Comput. Physics* 151:190–211
 25. Halperin A. 1999. Polymer brushes that resist adsorption of model proteins. *Langmuir* 15:2525–33
 26. Heinz WF, Hoh JH. 1999. Relative surface charge density mapping with the atomic force microscope. *Biophys. J.* 76:528–38
 27. Helm CA, Knoll W, Israelachvili JN. 1991. Measurement of ligand-receptor interactions. *Proc. Natl. Acad. Sci. USA* 88:8169–73
 28. Honig B, Nicolls A. 1995. Classical electrostatics in biology and chemistry. *Science* 268:1144–49
 29. Hunter R. 1989. *Foundations of Colloid Science*. Oxford, UK: Oxford Univ. Press
 30. Israilewitz B, Israilev S, Schulten K. 1997. Binding pathway of retinal to bacteriorhodopsin: a prediction by molecular dynamics simulations. *Biophys. J.* 73:2972–79
 31. Israelachvili J. 1992. Adhesion forces between surfaces in liquids and condensable vapours. *Surf. Sci. Rep.* 14:110–59
 32. Israelachvili J. 1992. *Intermolecular and Surface Forces*. New York: Academic
 33. Israelachvili J, Wennerström H. 1996. Role of hydration and water structure in biological and colloidal interactions. *Nature* 379:219–25
 34. Izrailev S, Stepaniants S, Balsera M, Oono Y, Schulten K. 1997. Molecular dynamics study of unbinding of the avidin-biotin complex. *Biophys. J.* 72:1568–81
 35. Jencks WP. 1987. *Catalysis in Chemistry and Enzymology*. Mineola, NY: Dover
 36. Jeon SI, Lee JH, Andrade JD, De Gennes PG. 1991. Protein-surface interactions in the presence of polyethylene oxide I: simplified theory. *J. Colloid Interface Sci.* 142:149–58
 37. Kaplanski G, Famarier C, Tissot O, Pierres A, Benoliel AM, et al. 1993. Granulocyte-endothelium initial adhesion: analysis of transient binding events mediated by E-selectin in a laminar shear flow. *Biophys. J.* 64:1922–33
 38. Kellermayer M, Smith SB, Granzier HL, Bustamante C. 1997. Folding-unfolding transitions in single titin molecules characterized with laser tweezers. *Science* 276:1112–15
 39. Kennedy MT, Kisak E, Trommshäuser D,

- Zasadzinski JA. 2000. Self-limiting aggregation by controlled ligand-receptor stoichiometry. Submitted
40. Khan S, Sheetz MP. 1997. Force effects on biochemical kinetics. *Annu. Rev. Biochem.* 66:785–805
 41. Koppenol W, Margoliash E. 1982. The asymmetric distribution of charges on the surface of horse heart cytochrome c. *J. Biol. Chem.* 257:4426–37
 42. Kramers HA. 1940. Brownian motion in a field of force and the diffusion model of chemical reactions. *Physica* 7:284–304
 43. Kuhl T, Leckband DE, Lasic DD, Israelachvili JN. 1995. Modulation of interaction forces between bilayers exposing short-chained ethylene oxide headgroups. *Biophys. J.* 66:1479–88
 44. Kuo SC, Lauffenburger DA. 1993. Relationship between receptor/ligand binding affinity and adhesion strength. *Biophys. J.* 65:2191–200
 45. Kuriyan J, O'Donnell M. 1993. Sliding clamps of DNA polymerases. *J. Mol. Biol.* 234:915–25
 46. Leckband DE, Kuhl TL, Wang HK, Müller W, Ringsdorf H. 1995. 4-4-20 Anti-fluorescyl IgG Fab' recognition of membrane bound hapten: direct evidence for the role of protein and interfacial structure. *Biochemistry* 34:11467–78
 47. Leckband D, Müller W, Schmitt F-J, Ringsdorf H. 1995. Molecular mechanisms determining the strength of receptor-mediated intermembrane adhesion. *Biophys. J.* 69:1162–69
 48. Leckband D, Schmitt F-J, Israelachvili J, Knoll W. 1994. Direct force measurements of specific and nonspecific protein interactions. *Biochemistry* 33:4611–24
 49. Lee GU, Kidwell DA, Colton RJ. 1994. Sensing discrete streptavidin-biotin interactions with atomic force microscopy. *Langmuir* 10:354–57
 50. Lu H, Isralewitz B, Krammer A, Vogel V, Schulten K. 1998. Unfolding of titin immunoglobulin domains by steered molecular dynamics simulation. *Biophys. J.* 75:662–71
 51. Lu H, Isralewitz B, Krammer A, Vogel V, Schulten K. 1998. Unfolding of titin immunoglobulin domains by steered molecular dynamics simulation. *Proc. Natl. Acad. Sci. USA* 75:662–71
 52. Matsui K, Boniface JJ, Reay PA, Hansjörg S, Fazekas de St. Groth B, Davis MM. 1991. Low-affinity interaction of peptide-MHC complexes with T-cell receptors. *Nature* 254:1788–91
 53. McCammon AJ. 1998. Theory of biomolecular recognition. *Curr. Opin. Struct. Biol.* 8:245–49
 54. Mehta A, Rief M, Spudich JA, Smith DA, Simmons RA. 1999. Single-molecule biomechanics with optical methods. *Science* 283:1689–95
 55. Merkel R, Nassoy P, Leung A, Ritchie K, Evans E. 1999. Energy landscapes of receptor-ligand bonds explored with dynamic force spectroscopy. *Nature* 397:50–53
 56. Moy VT, Florin E-L, Gaub HE. 1994. Intermolecular forces and energies between ligands and receptors. *Science* 266:257–59
 57. Müller DJ, Engel A. 1997. The height of biomolecules measured with the atomic force microscope depends on electrostatic interactions. *Biophys. J.* 73:1633–44
 58. Needham D, McIntosh TJ, Lasic D. 1992. Repulsive interactions and mechanical stability of polymer-grafted lipid membranes. *Biochim. Biophys. Acta* 1108:40–48
 59. Noppl-Simson DA, Needham D. 1996. Avidin-biotin interactions at vesicle surfaces: adsorption and binding, cross-bridge formation, and lateral interactions. *Biophys. J.* 70:1391–401
 60. Palecek S, Loftus JC, Ginsberg MH, Lauffenburger DA, Horwitz AF. 1997. Integrin-ligand binding properties govern cell migration speed through cell-substratum adhesiveness. *Nature* 385:537–40
 61. Papahadjopoulos D, Allen T, Gabizon A, Mayhew E, Matthay K, et al. 1991.

- Sterically stabilized liposomes: improvements in pharmacokinetics and antitumor therapeutic efficacy. *Proc. Natl. Acad. Sci. USA* 88:11460–64
62. Pierres A, Benoliel AM, Bongrand P. 1995. Measuring the lifetime of bonds made between surface-linked molecules. *J. Biol. Chem.* 270:26586–92
63. Pierres A, Benoliel AM, Bongrand P, Van Der Merwe AP. 1996. Determination of the lifetime and force dependence of interactions of single bonds between surface-attached CD2 and CD48 adhesion molecules. *Proc. Natl. Acad. Sci. USA* 93:15114–18
64. Rao Y, Wu X-F, Garipey J, Rutishauser U, Siu C-H. 1992. Identification of a peptide sequence involved in homophilic binding in the neural cell adhesion molecule NCAM. *J. Cell Biol.* 118:937–49
65. Rief M, Gautel M, Oesterhelt F, Fernandez JM, Gaub HE. 1999. Reversible unfolding of individual titin immunoglobulin domains by AFM. *Science* 276:1109–12
66. Rief M, Pascual J, Saraste M, Gaub HE. 1999. Single molecule force spectroscopy of spectrin repeats: low unfolding forces in helix bundles. *J. Mol. Biol.* 286:553–61
67. Rutishauser U. 1996. Polysialic acid and the regulation of cell interactions. *Curr. Opin. Cell Biol.* 8:679–84
68. Sabri S, Pierres A, Benoliel AM, Bongrand P. 1995. Influence of surface charges on cell adhesion: difference between static and dynamic conditions. *Biochem. Cell Biol.* 73:411–20
69. Saterbak A, Lauffenburger DA. 1996. Adhesion mediated by bonds in series. *Biotechnol. Prog.* 12:682–99
70. Sharp KA, Honig B. 1990. Electrostatic interactions in macromolecules: theory and applications. *Annu. Rev. Biophys. Biophys. Chem.* 19:302–32
71. Sterbe RE, Sheetz M. 1998. Basic laser tweezers. *Methods Cell Biol.* 55:29–41
72. Sheth SR, Leckband D. 1997. Measurements of attractive forces between proteins and end-grafted poly(ethylene glycol) chains. *Proc. Natl. Acad. Sci. USA* 94:8399–404
73. Shtilerman M, Lorimer GH, Englander W. 1999. Chaperonin function: folding by forced unfolding. *Science* 284:822–24
74. Simson DA, Strigl M, Hohenadl M, Merkle R. 1999. Statistical breakage of single protein A-IgG bonds reveals crossover from spontaneous to force-induced bond dissociation. *Phys. Rev. Lett.* 83:652–55
75. Sivasankar S, Briehner W, Lavrik N, Gumbiner B, Leckband D. 1999. Direct molecular force measurements of multiple adhesive interactions between cadherin ectodomains. *Proc. Natl. Acad. Sci. USA* 96:11820–24
76. Sivasankar S, Subramaniam S, Leckband D. 1998. Direct molecular level measurements of the electrostatic properties of a protein surface. *Proc. Natl. Acad. Sci. USA* 95:12961–66
77. Svoboda K, Block SM. 1994. Biological applications of optical forces. *Annu. Rev. Biophys. Biomolec. Struct.* 23:247–85
78. Szleifer I. 1997. Protein adsorption on surfaces with grafted polymers: a theoretical approach. *Biophys. J.* 72:595–12
79. Tees DF, Coenen O, Goldsmith HL. 1993. Interaction forces between red cells agglutinated by antibody. IV. Time and force dependence of break up. *Biophys. J.* 65:1318–34
80. Torney DC, Dembo M, Bell GI. 1986. Thermodynamics of cell adhesion. II. Freely mobile repellers. *Biophys. J.* 49:501–7
81. Tskhovrebova L, Trinick J, Sleep JA, Simmons RM. 1999. Elasticity and unfolding of single molecules of the giant muscle protein titin. *Nature* 387:308–12
82. Van Der Merwe PA, Brown MH, Davis S, Barclay NA. 1993. Affinity and kinetic analysis of the interaction of the cell adhesion molecules rat CD2 and CD48. *EMBO J.* 12:4945–54
83. Vinckier A, Gervasoni P, Zaugg F, Ziegler

- U, Lindner P, et al. 1998. Atomic force microscopy detects changes in the interaction forces between GroEL and substrate proteins. *Biophys. J.* 74:3256–63
84. Vijayendran R, Hammer D, Leckband D. 1998. Simulations of the adhesion between molecularly bonded surfaces in direct force measurements. *J. Chem. Phys.* 108:7783–93
85. Warshel A, Papazyan A. 1998. Electrostatic effects in macromolecules: fundamental concepts and practical modeling. *Curr. Opin. Struct. Biol.* 8:211–17
86. Wong JY, Kuhl TL, Israelachvili JN, Mullah N, Zalipsky S. 1997. Direct measurement of a tethered ligand-receptor interaction potential. *Science* 275:820–22
87. Yeung C, Leckband D. 1997. Molecular-level characterization of microenvironmental influences on the properties of immobilized proteins. *Langmuir* 13:6746–54
88. Yeung C, Purves T, Kloss A, Sligar S, Leckband D. 2000. Cytochrome c recognition of immobilized, orientational variants of cytochrome b5: direct force and equilibrium binding measurements. *Langmuir*. In press
89. Yip CM, Yip CC, Ward MD. 1998. Direct force measurements of insulin monomer-monomer interactions. *Biochemistry* 37:5439–49
90. Zhifeng S, Mou J, Czajkowsky DM, Yang J, Yuan JY. 1996. Biological atomic force microscopy: what is achieved and what is needed. *Adv. Physics.* 45:1–86